AN IMPROVEMENT OF OFFSET TRACKING FOR CROSS HAIR (CH) AND PATCH LIKE (PL) ELIMINATION AND RELIABILITY ESTIMATION FOR LARGE DEFORMATION MONITORING WITH SAR DATA

Sen Du, Jordi J. Mallorqui

CommSensLab, Universitat Politecnica de Catalunya (UPC), Barcelona, Spain

ABSTRACT

SAR based offset tracking (OT) is an efficient tool for ground deformation observation, and signal-noise-ratio (SNR) is its common error indicator. However, ground feature variation often weakens the accuracy of OT. In addition, SNR shows the signal reliability instead of result accuracy. Based on amplitude selection, cubic spline interpolation and double offset detecting, an improved OT method has been proposed in this paper. Subsidence caused by mining and GPS data have been employed to evaluate the performance of this scheme with TerraSAR-X data. The results indicate that PL and CH are reduced efficiently, and the error estimated by the proposed method has a higher correlation with real error than SNR in the mountainous area.

Index Terms— Offset tracking, error estimation, cross hair and patch like, SAR, ground deformation detection

1. INTRODUCTION

By detecting the offset of the pixels in the two images before and after the deformation, OT can obtain the surface deformation. A reference window is selected from the image acquired before the deformation. Then a moving search window from the image acquired after deformation is used to match the reference window. After the most similar search window is found, the offset between two images can be obtained.

Remotely sensed data makes it to be an extraordinary geodetic approach for large-scale deformation measurement. Among all kinds of sensors, SAR has proven its unprecedented ability and merits of withstanding severe weather conditions, making SAR acquisitions robust for OT technology [1, 2].

However, amplitude variations remain one of the major limitations for the retrieval of deformation signals from SAR stacks. On the one hand, the characteristic changes of the scatters could result in the amplitude value to change, causing noises shaped like thin lines, i.e. CH. On the other hand, the correlation overestimation of reference and search window due to amplitude weighted leads to the patch noise appearing in the result, i.e. PL. CH and PL make it difficult to retrieve the distributed deformation.

On the other side, numerous methods have been explored to estimate OT accuracy, and most of them are based on the maximum, mean and minimum values of correlation coefficient. However, it should be noted that high correlation coefficient represents reliability instead of accuracy.

In this paper, an amplitude filtering is proposed to reduce PL and CH. In addition, based on a double detection [1] and resampling [2], a new error estimating algorithm is introduced. To verify the advantages and feasibility of the scheme, it has been tested with GPS and TerraSAR-X data.

The paper is organized as follows. Section II details the scheme. The performance of the proposed method is evaluated by TerraSAR-X data in Section III. Finally, conclusions are given in Section IV.

2. PROPOSED METHOD

The proposed scheme is shown in Fig. 1 (a). Similar to traditional OT, the proposed method mainly consists of coarse registration [3], offset detection and error estimation. First of the two differences is, the primary image and the secondary image are pre-processed with amplitude filtering before the offset detection. The scheme of the amplitude filtering is shown in Fig. 1 (b). The purpose of this step is to eliminate the influence of CH and PL. Second, unlike the traditional OT that uses SNR or STD as error indicators, a new error estimation method based on double offset detection and cubic spline interpolation, named as rubber sheet (RB), is proposed. The steps of it are shown in Fig. 4.
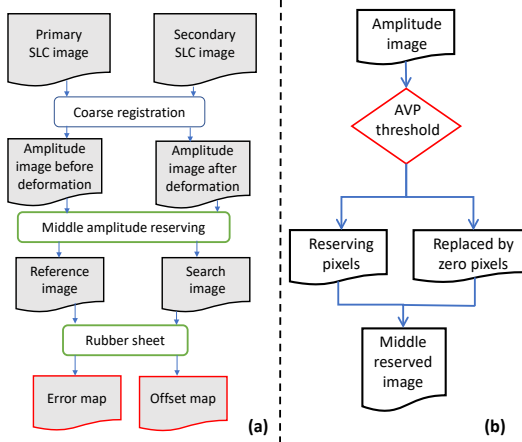
Fig. 1. Scheme of the proposed OT.(a)Overall scheme of the OT process. (b) Subscheme of the amplitude filtering.

Fig. 2. Relationship between errors and amplitude boundaries.

2.1. Amplitude filtering

Cross correlation is the key step to retrieve the pixel offset in two images. For the convolution operation, cross correlation coefficient is affected by amplitude weighting. If there is one or several pixels with very high amplitude in the primary image, and the amplitude value or position of these pixels changes in the secondary image, then when the matching window slides in the secondary image, the peak value of correlation coefficient will always appear at the position of the high-amplitude pixel in the primary image, which is the reason of PL. The characteristic of scatters with low amplitude is easy to change, causing the image feature to be inconspicuous, which is the reason of CH.

Therefore, in order to reduce PL and CH, pixels with very high and low amplitude need to be removed. To determine the threshold of the proposed amplitude filter, a part of the data introduced in Section III with no offsets are selected for an OT experiment, and the average value of the detected offset is regarded as the error. Different amplitude scales are selected to investigate the relationship between the amplitude range and error.

Two sets of experiments are carried out. In the first set of experiments, the lower boundary of amplitude scales is fixed to 0, the upper boundary increases from 90 to 810, and the step size is 30. In the second set of experiments, the upper boundary of amplitude scales is fixed to 410 according to the minimum error obtained in the first set of experiment, the lower boundary increases from 0 to 180, and the step size is 10. The relationship between the amplitude boundaries and the error are shown in Fig. 2.

It can be seen that the minimum errors are obtained when the lower boundary is 57 and the upper boundary is 410. The error comes mainly from CH and PL when the lower boundary is below 57 and upper boundary is beyond 410. Con-
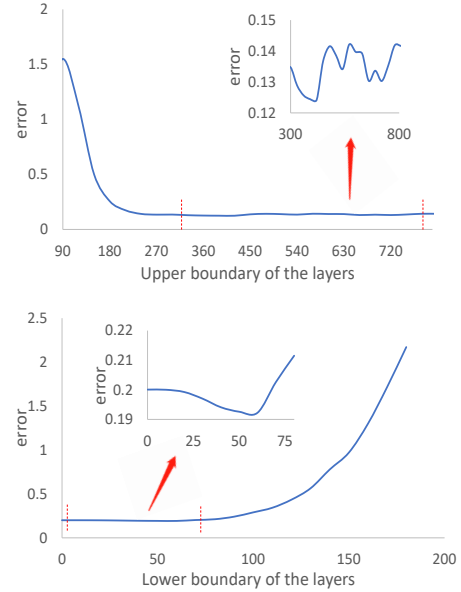
versely, when the lower boundary is beyond 57 and upper boundary is below 410, the error source is the insufficient amplitude roughness and missing information. Since the amplitude distribution obeys the Rayleigh distribution [4], and the scale parameter σ of the Rayleigh distribution is 60, σ is recommended to be set as the lower boundary, and the upper boundary is set to ρ. ρ is the threshold that can make the number of the retained pixels accounts for 60% of all pixels. The reason we set the lower boundary as a fixed value instead of the upper boundary, is that the possibility density in lower area is high, a fixed lower boundary can define the amplitude range more accurately. By establishing the relationship between the amplitude thresholds and σ, the transferability of the method can be improved. The amplitude filtering is described by (1) and Fig. 3.

$$A_{F(i,j)} = \begin{cases} A_{(i,j)}, & \sigma \leq A_{(i,j)} \leq \sigma + 350 \\ 0, & A_{(i,j)} \leq \sigma \ or \ A_{(i,j)} \geq \sigma + 350 \end{cases} \quad (1)$$

Where $A_{(i,j)}$ is an arbitrary pixel in the original amplitude image and $A_{F(i,j)}$ is its corresponding pixel in the filtered image.

After replacing the amplitude value of the discarded pixels in the original amplitude map with 0, the filtered image can be obtained.

2.2. Error estimation

Inspired by Scambos and Yun [1, 2], an OT error estimation method is proposed in this paper, as it is shown in Fig. 4.
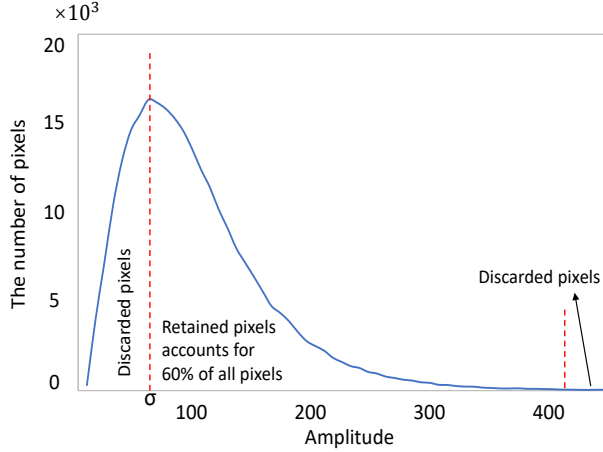
Fig. 3. Relationship between errors and amplitude boundaries.

First, the pixel offset between the reference and search images is obtained by OT. Afterwards, the search image is resampled in the slant-range direction according to the offset, the shifted pixels are corrected to the position before the deformation. Finally, OT is applied again to detect the offset between reference image and the resampled search image. The offset obtained in the second time is regarded as the error. The rationale is that if the first OT detection result deviates greatly from the real situation, there will still be offset between the pixels of the reference image and the corrected search image, and the second OT can detect this offset.
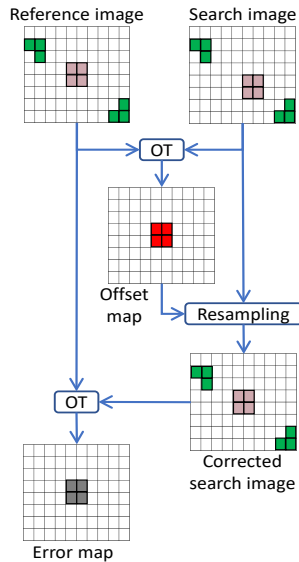

Fig. 4. Subscheme of rubber sheet. the green area represents the stable area, the pink area stands for the deformation area, the red area indicates the deformation detected by OT, and the gray area means the error.

3. RESULTS

A small area with deformation caused by the underground coal mining is used to assess the performance of the proposed method. The area of interest is located in Daliuta (China). The coal seam is thick, the burial is shallow, which leads to large deformation on the ground that beyond InSAR monitoring capability. The mining activity started on November 27, 2012 and finished on March 25, 2013. Two TSX SLC images with the spotlight imaging mode, pixel spacing of 0.91×0.86 m, spatial baseline of 35 m, incidence angle of $42.4°$, are employed to monitor the deformation. The master image is acquired on December 13, 2012 and the slave image on March 22, 2013. The region of interest (ROI) is chosen around the working mine, corresponding 1370 pixels in range and 1168 pixels in azimuth of the SAR images. There are 70 GPS stations, including 44 along the mining direction and 26 along the vertical mining direction, used for the validation.
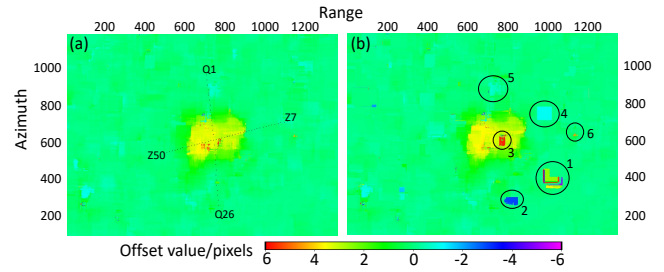

Fig. 5. The offsets in range direction obtained by the proposed method (a) and the conventional OT (b). The positive offset value means the movement away from the sensor, which is subsidence. The negative offset value means uplift. The small black dots in (a) indicate the locations of GPS stations. 'Z7', 'Z50', 'Q1' and 'Q26' are the names of the four GPS stations.

The offsets along range direction over the test area obtained by the two methods are shown in Fig. 5. As the figure shows, the shape and size of the subsidence basins obtained by the two methods are very similar, but the proposed method can effectively eliminate PL effects highlighted in the black circle $1 - 6$. Fig. 6 shows the amplitude images in black circle 1 and their correlation map. (a) and (b) show the pair of images before and after the deformation without amplitude filtering, (e) is their correlation map. (c) and (d) show the same pair of images with amplitude filtering, (f) is their correlation map. It can be seen that the offset of correlation coefficient is caused by a ground scatter feature change in the middle of the amplitude in Fig. 6 (b). After the amplitude filtering, other stable scatter feature dominate the correlation, so the peak appears in the center. Although the correlation coefficient is reduced, the amplitude filtering avoids the influence of unexpected ground feature changes.

To quantitatively analyse the two error detection methods, a simple linear regression analysis is carried out. The offset
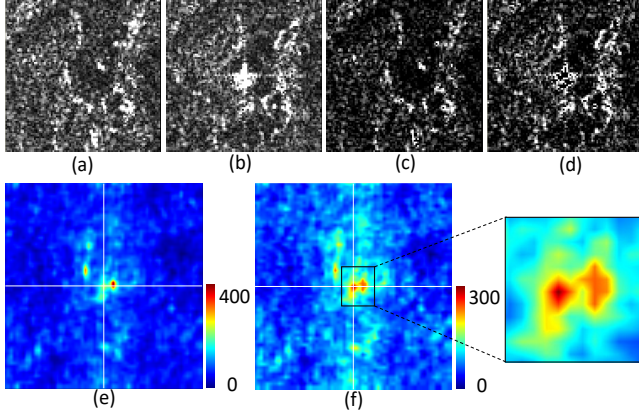
Fig. 6. Comparison between the amplitude image before and after amplitude filtering. (a) and (b) show the pair of images before and after the deformation without amplitude filtering, (e) is their correlation map. (c) and (d) show the same pair of images with amplitude filtering, (f) is their correlation map. White lines in the middle of (e) and (f) help locate the peak.

is first transformed into vertical by:

$$P_{\text{offset}} = \frac{S_{\text{sub}} \cdot \cos\theta}{R_{\text{size}}} \tag{2}$$

where P_{offset} is the pixel offset in range direction, S_{sub} the vertical deformation, θ the incident angle and R_{size} the pixel size in range direction. In this equation, the azimuth movement is ignored because it has no contribution to the vertical deformation.

The difference between GPS and OT result is considered as the real error. The average offset of 9 pixels closest to each GPS station is regarded as the final results. Because SNR cannot be directly compared with the real error, the SNR values are normalized according to:

$$S_{new} = \frac{S_{max} - S}{S_{max} - S_{min}} \cdot G_{max} \tag{3}$$

where S_{new} is the normalized SNR value, S_{max} is the maximum value in SNR map, S_{min} is the minimum value in SNR map, S is the SNR value before normalized and G_{max} is the maximum value of real error. In Fig. 7 (a), the error detected by RB increases as the true error increases. In Fig. 7 (b), however, the correlation between SNR error and real error is not obvious. R^2 also shows that the RB error has a higher correlation with real error than the SNR error.

4. CONCLUSION

In this paper, a new offset tracking strategy is proposed. Detailed comparison analyses between conventional OT and the proposed scheme has been carried out over Daliuta with TSX and GPS data. By amplitude filtering, the accuracy of OT is
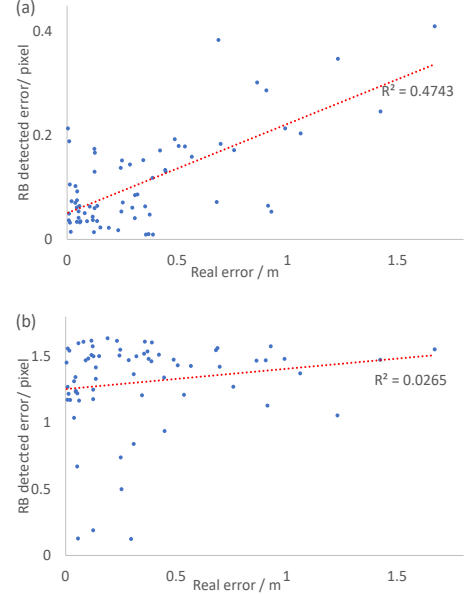

Fig. 7. Correlation between real error and error detected by RB (a) and SNR (b).

improved by reducing the impact of CH and PL. Compared with traditional correlation coefficient based error estimation methods such as SNR and STD, the proposed error estimating method is a result based algorithm, therefore, it can effectively avoid the influence of high amplitude contrast like layover, foreshortening and shadow.

5. REFERENCES

[1] Theodore A Scambos, Melanie J Dutkiewicz, Jeremy C Wilson, and Robert A Bindschadler, "Application of image cross-correlation to the measurement of glacier velocity using satellite image data," *Remote sensing of environment*, vol. 42, no. 3, pp. 177–186, 1992.

[2] Sang-Ho Yun, Howard Zebker, Paul Segall, Andrew Hooper, and Michael Poland, "Interferogram formation in the presence of complex and large deformation," *Geophysical Research Letters*, vol. 34, no. 12, 2007.

[3] Eugenio Sansosti, Paolo Berardino, Michele Manunta, Francesco Serafino, and Gianfranco Fornaro, "Geometrical sar image registration," *IEEE Transactions on Geoscience and Remote Sensing*, vol. 44, no. 10, pp. 2861–2870, 2006.

[4] Athanasios Papoulis and S Unnikrishna Pillai, *Probability, random variables, and stochastic processes*, Tata McGraw-Hill Education, 2002.